

# Heat transfer between a circular free impinging jet and a solid surface with non-uniform wall temperature or wall heat flux—2. Solution for the boundary layer region

X. S. WANG, Z. DAGAN and L. M. JIJI

Department of Mechanical Engineering, The City College of the City University of New York,  
Convent Ave. and 138th Street, New York, NY 10031, U.S.A.

(Received 9 May 1988 and in final form 28 November 1988)

**Abstract**—The heat transfer in the boundary layer region of a circular free jet impinging on a flat solid surface with non-uniform wall temperature or wall heat flux is investigated analytically. The flow is laminar, incompressible and steady. The analysis begins with obtaining the solution to the problem with a step change in wall temperature or wall heat flux. The solution to the corresponding problem with arbitrary wall temperature or wall heat flux is obtained by superposition. This solution is then matched with that for the stagnation region obtained in the first part of this study so that the Nusselt number throughout the stagnation region and the boundary layer region is obtained. The results indicate that the Nusselt number for increasing wall temperature or wall heat flux can be considerably higher than that for constant wall temperature or wall heat flux outside the stagnation region. For the special case of constant wall temperature, the result is in good agreement with the integral solution of Chaudhury.

## 1. INTRODUCTION

THIS is the second part of an analytical investigation of heat transfer between an axisymmetrical free impinging jet and a solid flat surface with non-uniform wall temperature or wall heat flux. The objective is to examine the heat transfer in the boundary layer region when a circular free jet impinges normally on a flat surface. It should be mentioned that the heat transfer of a free impinging jet is not the same as that of a submerged impinging jet since the flow field is different for the two cases.

The heat transfer between a laminar, circular impinging jet and a flat solid surface has been examined by a number of investigators. Chaudhury [1] investigated the heat transfer in the boundary layer region and similarity region. His solution is based on the velocity distribution obtained by Watson [2]. In his paper, the stagnation region is ignored. An integral solution was obtained in the boundary layer region and a similarity solution to the energy equation was given in the similarity region. He considered two specific cases. In the first case the wall is thermally insulated for  $r \leq r_s$  and is maintained at a constant temperature which is different from that of the jet at  $r > r_s$ , where  $r = r_s$  is located in the similarity region. In the second case the wall is maintained at a constant temperature throughout. Brdlik and Savin [3] solved the heat transfer problem of jet impingement with constant wall temperature by the integral method and also obtained experimental results. Their integral solution is based on the assumption that the ratio of thermal boundary layer thickness to viscous boundary

layer thickness is  $1/Pr^{1/3}$  and the local heat transfer coefficient was not given in their experimental work. Saad *et al.* [4] numerically examined heat transfer from a laminar, semi-confined axisymmetric submerged impinging jet. They used an upwind finite-difference representation of the momentum and energy equations to predict the flow and local heat transfer characteristics of a laminar round jet impinging normally on a flat wall. Laminar jet impingement heat transfer including the effects of melting was considered by Lipsett and Gilpin [5]. The solution of the potential flow problem was obtained by the finite-element method and the boundary layer problem was solved by the Karman-Pohlhausen integral method. When there is no effect of melting, the results show that a maximum in the heat transfer distribution exists near  $r = r_0$ , where  $r_0$  is the jet radius.

Heat transfer of submerged wall jets was investigated analytically by Mitachi and Ishiguro [6]. They obtained similarity solutions to the energy equation for the boundary conditions of an isothermal wall, a uniform wall heat flux and an adiabatic wall. For the case of a step change in the wall temperature, the energy equation is solved numerically.

## 2. FORMULATION

In the boundary layer region (see Fig. 1 in Part 1 of this study), radial convection is much more important than the radial conduction and hence the temperature field is of the boundary layer type. For such a flow, the energy equation is

## NOMENCLATURE

$a_2, a_5, a_8, a_{11}$	constants defined in equations (4)	$U_0$	jet velocity
$b$	constant defined in equation (14a)	$w$	velocity in the $z$ -direction
$d$	jet diameter	$z$	coordinate normal to the wall.
$e_1, e_2$	coefficients defined in equations (14b) and (14c)	Greek symbols	
$f$	dimensionless function, equation (4a)	$\alpha$	diffusivity
$k$	conductivity	$\delta$	boundary layer thickness defined in equation (6)
$Nu$	Nusselt number, $Q_w d/k(T_w - T_\infty)$	$\delta'$	boundary layer thickness defined in equation (7)
$Pr$	Prandtl number	$\eta$	dimensionless variable defined in equation (5)
$Q_w$	heat flux on the wall	$\theta_{ca}$	dimensionless temperature defined in equation (50)
$r$	coordinate along the wall	$\theta_{sq}$	dimensionless temperature defined in equation (26)
$r_0$	jet radius	$\theta_{st}$	dimensionless temperature defined in equation (9)
$R$	dimensionless coordinate defined in equations (10)	$\nu$	kinematic viscosity
$Re$	Reynolds number, $U_0 d/\nu$	$\xi$	dimensionless variable defined in equation (10).
$T$	temperature		
$T_w$	wall temperature		
$T_\infty$	jet temperature or temperature outside the thermal boundary layer		
$u$	velocity in the $r$ -direction		

$$u \frac{\partial T}{\partial r} + w \frac{\partial T}{\partial z} = \alpha \frac{\partial^2 T}{\partial z^2} \quad (1)$$

and the boundary conditions are

$$T = T_w(r) \quad \text{or} \quad Q = Q_w(r) \quad \text{at} \quad z = 0 \quad (2a)$$

$$T = T_\infty \quad \text{at} \quad z = \infty \quad (2b)$$

where  $T_\infty$  is the jet temperature,  $T_w(r)$  the wall temperature, and  $Q_w(r)$  the wall heat flux. The velocity components  $u$  and  $w$  are obtained from the solution to the flow field [2]

$$u = U_0 f'(\eta) \quad (3a)$$

$$w = \frac{\nu}{z} \left( -\eta f + \frac{\eta^2}{3} f' \right) \quad (3b)$$

where  $f$  is defined by a third-order ordinary differential equation and can be expanded in the following form:

$$f = a_2 \eta^2 + a_5 \eta^5 + a_8 \eta^8 + a_{11} \eta^{11} + \dots \quad (4a)$$

$$a_2 = 0.23480, \quad a_5 = -0.18377 \times 10^{-2} \quad (4b)$$

$$a_8 = 0.28252 \times 10^{-4}, \quad a_{11} = -0.45686 \times 10^{-6}. \quad (4c)$$

The primes in equations (3) denote differentiation with respect to  $\eta$  which is defined as

$$\eta = \sqrt{\left( \frac{3U_0}{2\nu r} \right) z}. \quad (5)$$

As was pointed out in ref. [2], the above solution is based on the assumption of  $r \gg r_0$  so that the conditions in the stagnation region do not affect the flow in the boundary layer region. To investigate the spatial range in which the above solution is applicable, we use the integral solution to examine the effect of the

conditions in the stagnation region on the flow in the boundary layer region. In Part 1 of this study, it was shown that the boundary layer thickness outside the stagnation region is given by

$$\delta = \sqrt{\left( \frac{420}{37} \frac{\nu}{U_0} r + \frac{c}{r^2} \right)} \quad (6)$$

where

$$c = 0.81 \frac{\nu}{U_0} r_0^3.$$

The term  $c/r^2$  represents the influence of the stagnation region on the boundary layer thickness in the boundary layer region. If this effect is neglected, the boundary layer thickness becomes

$$\delta' = \sqrt{\left( \frac{420}{37} \frac{\nu}{U_0} r \right)}. \quad (7)$$

Comparison between equations (6) and (7) shows that for  $r \geq 2r_0$ , the influence of the stagnation region on the boundary layer thickness in the boundary layer region is smaller than 0.5%. It follows that solution (3) is valid for  $r \geq 2r_0$  with negligible error.

## 3. SOLUTIONS

Because of the linearity of energy equation (1), it is possible to obtain the solution by the superposition method. We seek a solution for the general case of arbitrary wall temperature or arbitrary wall heat flux. As shown in Fig. 1, an arbitrary wall temperature distribution  $T_w(r)$  or wall heat flux distribution  $Q_w(r)$

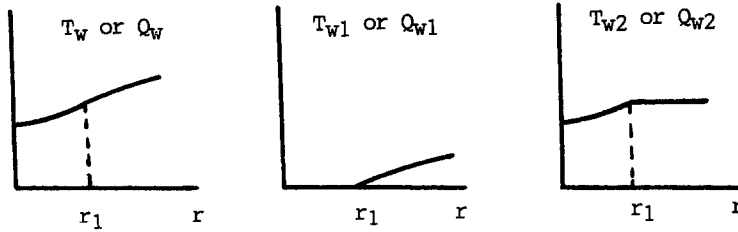


FIG. 1. Division of arbitrary wall temperature or wall heat flux.

may be divided into two parts. In the first part, the wall temperature or wall heat flux is

$$T_{w_1} = T_w(r) - T_w(r_1)$$

or

$$Q_{w_1} = Q_w(r) - Q_w(r_1)$$

for  $r > r_1$  and is zero for  $r \leq r_1$ . In the second part, the wall temperature or wall heat flux is  $T_{w_2} = T_w(r)$  or  $Q_{w_2} = Q_w(r)$  for  $r \leq r_1$  and is  $T_{w_2} = T_w(r_1)$  or  $Q_{w_2} = Q_w(r_1)$  for  $r > r_1$ . It follows that the temperature distribution in the boundary layer region for  $r > r_1$  can also be divided into two parts. We will proceed by first obtaining the solution to the problem with a step change in wall temperature or wall heat flux. Then we obtain the solutions to the problem with  $T_w = T_{w_1}$  or  $Q_w = Q_{w_1}$  and  $T_w = T_{w_2}$  or  $Q_w = Q_{w_2}$  as shown in the figure. Finally, the solution to the problem with arbitrary wall temperature or wall heat flux is obtained by superposition.

### 3.1. Solution for a step change in wall temperature

In this section, we consider the case where part of the wall,  $r \leq r^*$ , is assumed to be thermally insulated and the rest maintained at a constant temperature  $T_1$ . The end point,  $r = r^*$ , of the thermally insulated part is located in the boundary layer region. Therefore, for  $r \leq r^*$  the wall temperature is uniform and equal to the fluid temperature which is assumed to be zero for convenience. Consequently, the boundary conditions are

$$T(r^*, z) = 0, \quad T(r, \infty) = 0, \quad T(r > r^*, 0) = T_1. \tag{8}$$

To write the energy equation and boundary conditions in dimensionless form, we introduce the following dimensionless temperature and coordinates:

$$\theta_{st} = \frac{T}{T_1} \tag{9}$$

and

$$R = 1 - \frac{r^*}{r}, \quad \xi = b \frac{\eta}{R^{1/3}} \tag{10}$$

where  $\eta$  is defined in equation (5) and  $b$  is a constant to be determined later. The dimensionless forms of

energy equation (1) and boundary conditions (8), therefore, become

$$\frac{\partial^2 \theta_{st}}{\partial \xi^2} + \left[ \frac{2Pr}{9b^2} \frac{1-R}{R^{1/3}} \xi f' + \frac{Pr}{b} R^{1/3} f \right] \frac{\partial \theta_{st}}{\partial \xi} - \frac{2Pr}{3b^2} R^{2/3} (1-R) f' \frac{\partial \theta_{st}}{\partial R} = 0 \tag{11}$$

and

$$\theta_{st}(R, 0) = 1, \quad \theta_{st}(R, \infty) = 0. \tag{12}$$

Transformation (10) has two advantages.

- (1)  $R$  is always less than unity. This is very important for obtaining a series solution in powers of  $R$ .
- (2) The boundary conditions at  $r = r^*$  and at  $z = \infty$  are merged into one, therefore the number of boundary conditions is reduced to two. Since  $R$  is bounded between 0 and 1, the dependent variable  $\theta_{st}$  can be expanded in a Taylor series as follows:

$$\theta_{st} = F_0(\xi) + F_1(\xi)R + F_2(\xi)R^2 + F_3(\xi)R^3 + \dots \tag{13}$$

Upon substituting equations (4), (10) and (13) into equation (11), comparing the coefficients of like power of  $R$  and introducing the following definitions:

$$b = \frac{(4a_2)^{1/3}}{3} Pr^{1/3} = 0.32644 Pr^{1/3} \tag{14a}$$

$$e_1 = \frac{10Pr a_5}{9b^6} = -1.6875 Pr^{-1} \tag{14b}$$

$$e_2 = \frac{16Pr a_8}{9b^9} = 1.1933 Pr^{-2} \tag{14c}$$

$$F_1 = F_{11} + e_1 F_{12} \tag{14d}$$

$$F_2 = e_1 F_{21} + e_2 F_{22} + F_{23} \tag{14e}$$

the governing ordinary differential equations and the boundary conditions for the universal functions  $F_0(\xi)$ ,  $F_{11}(\xi)$ ,  $F_{12}(\xi)$ ,  $F_{21}(\xi)$ ,  $F_{22}(\xi)$  and  $F_{23}(\xi)$ , are obtained as follows:

$$F_0'' + 3\xi^2 F_0' = 0 \tag{15a}$$

$$F_0(0) = 1, \quad F_0(\infty) = 0 \tag{15b}$$

$$F_{11}'' + 3\xi^2 F_{11}' - 9\xi F_{11} = -\frac{1}{4} \xi^2 F_0' \tag{16a}$$

$$F_{11}(0) = F_{11}(\infty) = 0 \tag{16b}$$

$$F''_{12} + 3\xi^2 F'_{12} - 9\xi F_{12} = -\xi^5 F'_0 \quad (17a)$$

$$F_{12}(0) = F_{12}(\infty) = 0 \quad (17b)$$

$$F''_{21} + 3\xi^2 F'_{21} - 18\xi F_{21} = 3\xi^4 F'_{11} - \xi^5 F'_{11} - 9\xi F_{12} - \frac{15}{4}\xi^2 F'_{12} + \frac{1}{10}\xi^5 F'_0 \quad (18a)$$

$$F_{21}(0) = F_{21}(\infty) = 0 \quad (18b)$$

$$F''_{22} + 3\xi^2 F'_{22} - 18\xi F_{22} = 2.3864(3\xi^4 F'_{12} - \xi^5 F'_{12}) - \xi^8 F'_0 \quad (19a)$$

$$F_{22}(0) = F_{22}(\infty) = 0 \quad (19b)$$

$$F''_{23} + 3\xi^2 F'_{23} - 18\xi F_{23} = -9\xi F'_{11} - \frac{15}{4}\xi^2 F'_{11} \quad (20a)$$

$$F_{23}(0) = F_{23}(\infty) = 0. \quad (20b)$$

The solution to equations (15) is clearly

$$F_0(\xi) = 1 - \frac{3}{\Gamma(1/3)} \int_0^\xi e^{-\eta^3} d\eta. \quad (21)$$

The remaining equations (16)–(20) are solved numerically and the results are shown graphically in Fig. 2. The associated wall derivatives are given in Table 1. With the information provided in Fig. 2 and Table 1, the temperature field and the wall heat flux can be easily determined. The wall heat flux is obtained by differentiating equation (13) as follows :

$$q_w = -k \sqrt{\left(\frac{3U_0}{2vr}\right)} \frac{b}{R^{1/3}} T_1 [F'_0(0) + F'_1(0)R + F'_2(0)R^2 + \dots]. \quad (22)$$

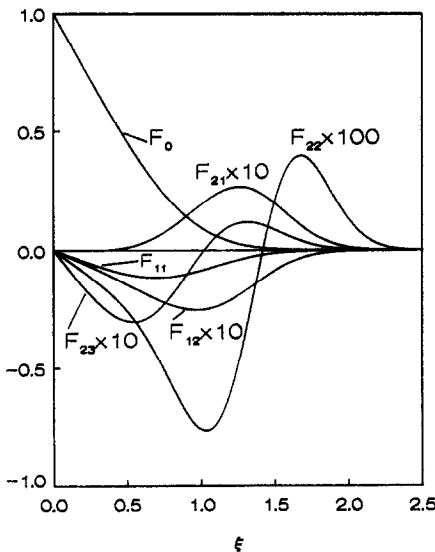


FIG. 2.  $F_{ij}$  functions for a step change in wall temperature.

Hence the Nusselt number is

$$Nu = -b Re^{1/2} \frac{\sqrt{\left(\frac{3d}{2r}\right)}}{(1-r^*/r)^{1/3}} [F'_0(0) + F'_1(0)(1-r^*/r) + F'_2(0)(1-r^*/r)^2 + \dots] \quad (23)$$

where  $b$  is given in equation (14a) and  $Re$  is the Reynolds number defined by  $U_0 d/\nu$ . The constants  $F'_0(0)$ ,  $F'_1(0)$  and  $F'_2(0)$  in the above equations are given by

$$F'_0(0) = -\frac{3}{\Gamma(1/3)} \quad (24a)$$

$$F'_1(0) = -0.23329 + 0.046658 Pr^{-1} \quad (24b)$$

$$F'_2(0) = -0.077764 + 0.0015553 Pr^{-1} - 0.0052878 Pr^{-2}. \quad (24c)$$

Obviously, the solution is valid for  $r > r^*$  only.

The calculation shows that for a Prandtl number of the order of unity or larger, solution (13) converges very fast and good accuracy is obtainable with terms of up to order 2. For fluids with very small Prandtl number such as liquid metal, however, the solution converges only when  $R$  is small. In such a case, Euler's transformation may be used for the evaluation of the sum. The Nusselt number profile is plotted in Fig. 3 for  $Pr = 0.7, 7$  and  $20$ .

### 3.2. Solution for a step change in wall heat flux

In this problem the prescribed wall heat flux is zero for  $r \leq r^*$  and  $q_1$  for  $r > r^*$  where  $r^*$  is located in the boundary layer region. Specifically, the boundary conditions are

$$T(r^*, z) = 0, \quad T(r, \infty) = 0,$$

$$-k \frac{\partial T(r > r^*, 0)}{\partial z} = q_1. \quad (25)$$

A dimensionless temperature  $\theta_{sq}$  is defined as follows :

$$\theta_{sq} = \frac{b\sqrt{(3U_0/2vr)}k}{q_1 R^{1/3}} T \quad (26)$$

where constant  $b$  is given by equation (14a). The specific form of equation (26) is motivated by the consideration that the transformed boundary condition on the wall is still a constant. The dimensionless form of energy equation (1) and boundary conditions (25) then become

Table 1. Wall derivatives

$F'_0(0)$	$F'_{11}(0)$	$F'_{12}(0)$	$F'_{21}(0)$	$F'_{22}(0)$	$F'_{23}(0)$
-1.1198	-0.23329	-0.027649	-0.00092164	-0.0044312	-0.077764

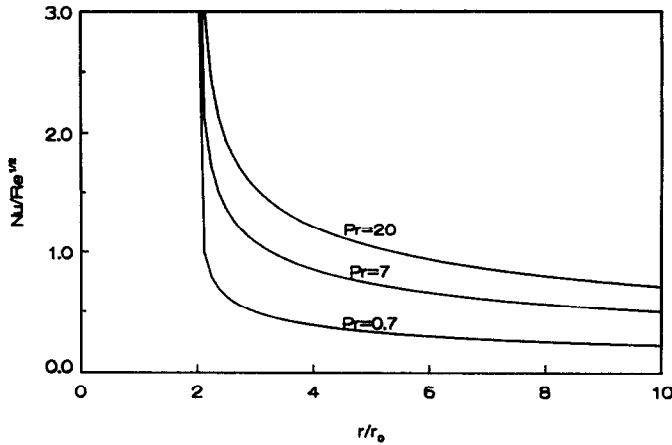


FIG. 3. Nusselt number profile for a step change in wall temperature.

$$\frac{\partial^2 \theta_{sq}}{\partial \xi^2} + \left[ \frac{2Pr}{9b^2} \frac{1-R}{R^{1/3}} \xi f' + \frac{Pr}{b} R^{1/3} f \right] \frac{\partial \theta_{sq}}{\partial \xi} - \frac{2Pr}{3b^2} R^{2/3} f' (1-R) \frac{\partial \theta_{sq}}{\partial R} - \frac{2Pr}{9b^2} R^{2/3} f' \left( \frac{1}{R} + \frac{1}{2} \right) \theta_{sq} = 0 \quad (27)$$

and

$$\frac{\partial \theta_{sq}}{\partial \xi} = -1 \quad \text{at } \xi = 0 \quad (28a)$$

$$\theta_{sq} = 0 \quad \text{at } \xi = \infty. \quad (28b)$$

Note that the only difference between equations (11) and (27) is that equation (27) has one additional term, i.e. the last term. Proceeding as with equation (13),  $\theta_{sq}$  can be written in the following form:

$$\theta_{sq} = B_0(\xi) + B_1(\xi)R + B_2(\xi)R^2 + B_3(\xi)R^3 + \dots \quad (29)$$

Following the same procedure as that in Section 3.1 and introducing the following definitions:

$$B_1 = e_1 B_{11} + B_{12} \quad (30a)$$

$$B_2 = e_2 B_{21} + e_1 B_{22} + B_{23} \quad (30b)$$

where  $e_1$  and  $e_2$  are given by equations (14), one obtains the following differential equations and the corresponding boundary conditions:

$$B_0'' + 3\xi^2 B_0' - 3\xi B_0 = 0 \quad (31a)$$

$$B_0'(0) = -1, \quad B_0(\infty) = 0 \quad (31b)$$

$$B_{11}'' + 3\xi^2 B_{11}' - 12\xi B_{11} = \xi^4 B_0 - \xi^5 B_0' \quad (32a)$$

$$B_{11}'(0) = B_{11}(\infty) = 0 \quad (32b)$$

$$B_{12}'' + 3\xi^2 B_{12}' - 12\xi B_{12} = -\frac{1}{4}\xi^2 B_0' + \frac{3}{2}\xi B_0 \quad (33a)$$

$$B_{12}'(0) = B_{12}(\infty) = 0 \quad (33b)$$

$$B_{21}'' + 3\xi^2 B_{21}' - 21\xi B_{21} = 2.3864(4\xi^4 B_{11} - \xi^5 B_{11}') - \xi^8 B_0' + \xi^7 B_0 \quad (34a)$$

$$B_{21}'(0) = B_{21}(\infty) = 0 \quad (34b)$$

$$B_{22}'' + 3\xi^2 B_{22}' - 21\xi B_{22} = 4\xi^4 B_{12} - \xi^5 B_{12}' - \frac{1}{2}\xi B_{11} - \frac{1}{4}\xi^2 B_{11}' + \frac{1}{10}\xi^5 B_0' + \frac{1}{2}\xi^4 B_0 \quad (35a)$$

$$B_{22}'(0) = B_{22}(\infty) = 0 \quad (35b)$$

$$B_{23}'' + 3\xi^2 B_{23}' - 21\xi B_{23} = -\frac{1}{2}\xi B_{12} - \frac{1}{4}\xi^2 B_{12}' \quad (36a)$$

$$B_{23}'(0) = B_{23}(\infty) = 0. \quad (36b)$$

The solution of equations (31) can be obtained in closed form

$$B_0(\xi) = \frac{1}{\Gamma(2/3)} \left[ e^{-\xi^3} + 3\xi \int_0^\xi \eta e^{-\eta^3} d\eta \right] - \xi \quad (37)$$

while equations (32)–(36) are solved numerically. Note that  $B_0, B_{11}, B_{12}, B_{21}, B_{22}, B_{23}$  and  $F_0, F_{11}, F_{12}, F_{21}, F_{22}, F_{23}$  in the previous section are independent of Prandtl number, and, therefore, have to be calculated only once. These functions are shown graphically in Fig. 4 and their values on the wall are given in Table 2. Finally, the wall temperature is given by

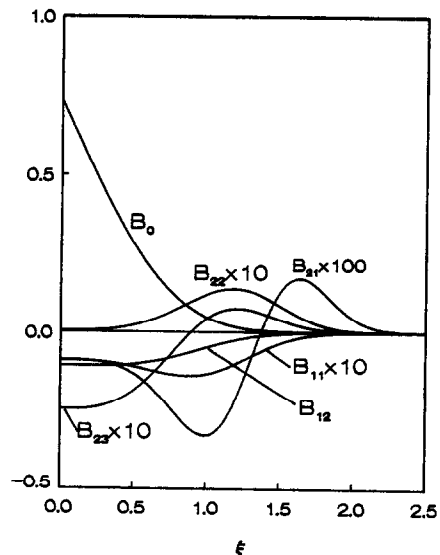


FIG. 4.  $B_j$  functions for a step change in wall heat flux.

Table 2.  $B_j$  values on the wall

$B_0(0)$	$B_{1,1}(0)$	$B_{1,2}(0)$	$B_{2,1}(0)$	$B_{2,2}(0)$	$B_{2,3}(0)$
0.73849	-0.0091171	-0.10770	-0.00089019	-0.00043415	-0.024726

$$T_w = \frac{q_1 R^{1/3}}{b \sqrt{\left(\frac{3U_0}{2\nu r}\right)k}} [B_0(0) + B_1(0)R + B_2(0)R^2 + \dots] \tag{38}$$

and the Nusselt number is

$$Nu = \frac{1}{(1-r^*/r)^{1/3}} \times \frac{b Re^{1/2} \sqrt{\left(\frac{3d}{2r}\right)}}{B_0(0) + B_1(0)(1-r^*/r) + B_2(0)(1-r^*/r)^2 + \dots} \tag{39}$$

where

$$B_0(0) = \frac{1}{\Gamma(2/3)} \tag{40a}$$

$$B_1(0) = -0.10770 + 0.015385 Pr^{-1} \tag{40b}$$

$$B_2(0) = -0.024726 - 0.00073263 Pr^{-1} - 0.0010623 Pr^{-2}. \tag{40c}$$

The Nusselt number profile is shown in Fig. 5 for  $Pr = 0.7, 7$  and  $20$ , respectively. The comparison of Fig. 5 with Fig. 3 shows that the Nusselt number profiles for a step change in wall temperature and for a step change in wall heat flux are similar, but the latter is a little higher. As  $r$  approaches  $r^*$ , the Nusselt number is singular because the wall temperature at  $r = r^*$  is assumed to be equal to the temperature outside the thermal boundary layer, as can be seen in boundary conditions (8) and (25). As a matter of fact,

the behavior of the Nusselt number profiles is similar to that of the Blasius flow over a flat plate with a constant wall temperature.

### 3.3. Solution for non-uniform wall temperature

We will now consider the case of a continuous wall temperature distribution  $T_w(r)$  with  $T_w(r) = 0$  for  $r \leq r_1$ , where  $r_1$  may be taken to be  $2r_0$  following the discussion of Section 2. The temperature outside the boundary layer is assumed to be zero. In Section 3.1, we have obtained the solution to the problem with a step change in wall temperature. For the problem with continuous wall temperature distribution  $T_w(r)$ , the solution can be obtained by the superposition method as follows:

$$T(r, z) = \int_{r_1}^r \theta_{st}(r, z, r^*) \frac{dT_w(r^*)}{dr} dr^*. \tag{41}$$

The wall heat flux is

$$q_w = -k \int_{r_1}^r \frac{\partial}{\partial z} \theta_{st}(r, 0, r^*) \frac{d}{dr} T_w(r^*) dr^* \tag{42}$$

where

$$\frac{\partial}{\partial z} \theta_{st}(r, 0, r^*) = \frac{b \sqrt{(3U_0/2\nu r)}}{(1-r^*/r)^{1/3}} \left[ F_0'(0) + F_1'(0) \left(1 - \frac{r^*}{r}\right) + F_2'(0) \left(1 - \frac{r^*}{r}\right)^2 + \dots \right]. \tag{43}$$

Consequently, the Nusselt number is

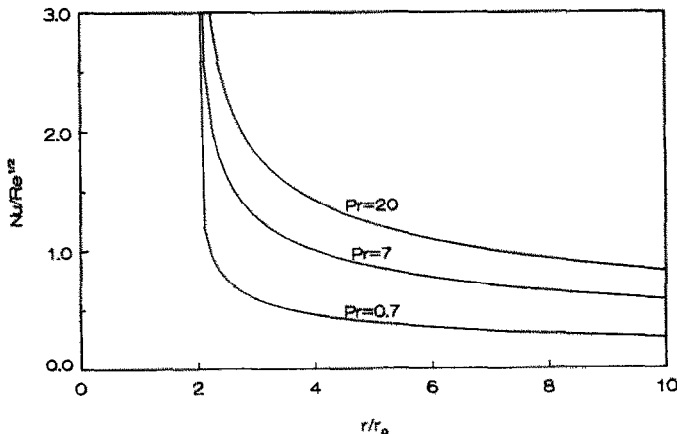


FIG. 5. Nusselt number profile for a step change in wall heat flux.

$$Nu = -\frac{b Re^{1/2} \sqrt{(3d/2r)}}{T_w(r)} \int_{r_1}^r \frac{1}{(1-r^*/r)^{1/3}} \times [F'_0(0) + F'_1(0)(1-r^*/r) + F'_2(0)(1-r^*/r)^2 + \dots] \frac{dT_w(r^*)}{dr} dr^* \quad (44)$$

where  $F'_0(0)$ ,  $F'_1(0)$  and  $F'_2(0)$  are given by equations (24). The Nusselt number profiles for different Prandtl numbers are shown in Fig. 6 for an increasing wall temperature which is also shown in the same figure in dimensionless form.

3.4. Solution for non-uniform wall heat flux

The wall heat flux is assumed to have a continuous distribution  $Q_w(r)$  with  $Q_w(r) = 0$  for  $r \leq r_1$ . Consequently, the wall temperature is  $T_w(r) = 0$  for  $r \leq r_1$  if the temperature outside the thermal boundary layer is assumed to be zero for convenience. The temperature distribution for  $r > r_1$  may be obtained from the corresponding solution for a step change in wall heat flux by the superposition method as follows :

$$T(r, z) = \frac{1}{b\sqrt{(3U_0/2vr)k}} \times \int_{r_1}^r (1-r^*/r)^{1/3} \theta_{sq}(r, z, r^*) \frac{dQ_w(r^*)}{dr} dr^* \quad (45)$$

where  $\theta_{sq}(r, z, r^*)$  is defined by equation (29). The wall temperature for  $r > r_1$  is

$$T_w = \frac{1}{b\sqrt{(3U_0/2vr)k}} \times \int_{r_1}^r (1-r^*/r)^{1/3} \theta_{sq}(r, 0, r^*) \frac{dQ_w(r^*)}{dr} dr^* \quad (46)$$

where

$$\theta_{sq}(r, 0, r^*) = B_0(0) + B_1(0)(1-r^*/r) + B_2(0)(1-r^*/r)^2 + \dots \quad (47)$$

and  $B_0(0)$ ,  $B_1(0)$ ,  $B_2(0)$  are given by equations (40). The Nusselt number can be obtained as follows :

$$Nu = b Re^{1/2} \sqrt{(3d/2r)} Q_w(r) \left\{ \int_{r_1}^r \left(1 - \frac{r^*}{r}\right)^{1/3} \left[ B_0(0) + B_1(0) \left(1 - \frac{r^*}{r}\right) + B_2(0) \left(1 - \frac{r^*}{r}\right)^2 + \dots \right] \frac{dQ_w(r^*)}{dr} dr^* \right\} \quad (48)$$

The Nusselt number profile is shown in Fig. 7 for an increasing wall heat flux with  $r$ . Comparing Figs. 6 and 7 with Figs. 3 and 5, one can see that the Nusselt number for continuously increasing wall temperature or wall heat flux is higher than that for a step change in wall temperature or wall heat flux. The reason is that at the same location, the fluid is hotter for the case of step change in wall temperature or wall heat flux than it is for the case of continuously increasing wall temperature or wall heat flux if the wall temperature or wall heat flux at that point is the same for both cases.

3.5. Solution to the problem with  $T_w = T_{w_2}$  and  $Q_w = Q_{w_2}$

Since the wall temperature or wall heat flux is constant for  $r > r_1$ , it is possible to obtain a similarity solution. For the case of prescribed wall heat flux, the boundary conditions are

$$-k \frac{\partial T}{\partial z} = Q_w(r_1) \quad \text{at } z = 0 \quad (49a)$$

$$T = T_\infty \quad \text{at } z = \infty. \quad (49b)$$

The dimensionless temperature  $\theta_{eq}$ , is now introduced as follows :

$$\theta_{eq} = \frac{T - T_\infty}{Q_w(r_1)} \sqrt{(3U_0/2vr)k}. \quad (50)$$

Energy equation (1) and boundary conditions (49), therefore, can be written as

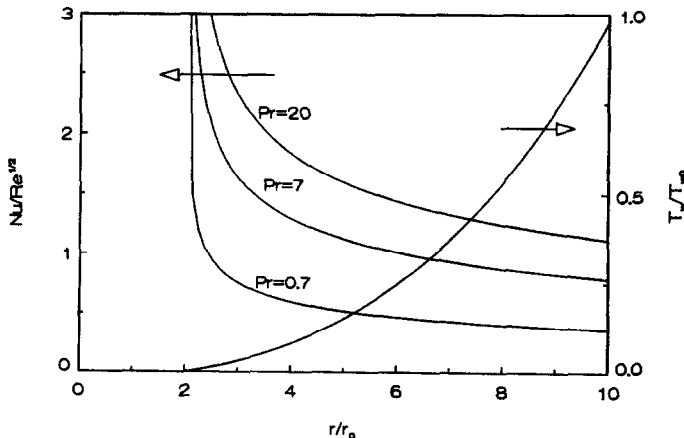


FIG. 6. Nusselt number profile for continuous wall temperature.

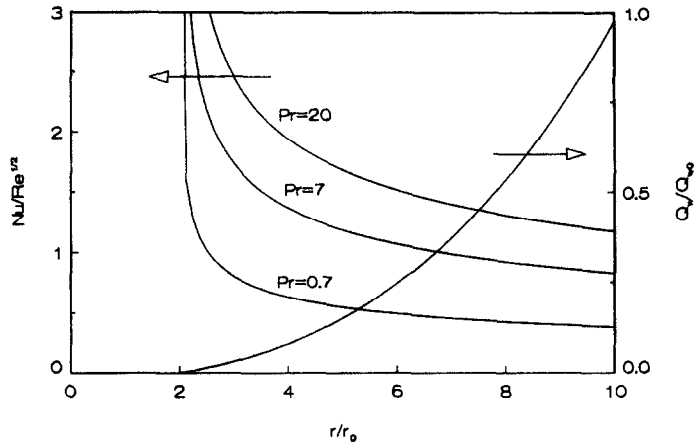


FIG. 7. Nusselt number profile for continuous wall heat flux.

$$\frac{d^2\theta_{cq}}{d\eta^2} + Pr f \frac{d\theta_{cq}}{d\eta} - \frac{Pr}{3} f' \theta_{cq} = 0 \quad (51a)$$

$$\theta'_{cq}(0) = -1, \quad \theta_{cq}(\infty) = 0 \quad (51b)$$

which may be solved numerically. Once  $\theta_{cq}$  is known, the temperature distribution corresponding to  $Q_w = Q_{w_2}$  is given by

$$T = T_\infty + \frac{Q_w(r_1)}{\sqrt{(3U_0/2\nu)r}k} \theta_{cq}. \quad (52)$$

For the case of prescribed wall temperature, the temperature distribution corresponding to  $T_w = T_{w_2}$  can be obtained by the same method as follows:

$$T = T_\infty + [T_w(r_1) - T_\infty] \times \left[ 1 - \frac{\int_0^\eta \exp\left[-Pr \int_0^\eta f d\eta\right] d\eta}{\int_0^\infty \exp\left[-Pr \int_0^\eta f d\eta\right] d\eta} \right]. \quad (53)$$

With the above solutions and those obtained in Sections 3.3 and 3.4, we are able to obtain the solutions for arbitrary wall temperature and wall heat flux.

3.6. Solution for arbitrary wall temperature

For Prandtl numbers larger than unity, the thermal boundary layer thickness is always smaller than the total thickness of the fluid layer in the boundary layer region. Consequently, the temperature outside the thermal boundary layer is the same as the jet temperature. Following the previous discussion, if the jet temperature is  $T_\infty$  and the wall temperature is  $T_w(r)$ , the temperature distribution in the boundary layer region should be the sum of equations (41) and (53) for  $r > r_1$ . That is

$$T = T_\infty + [T_w(r_1) - T_\infty] \times \left[ 1 - \frac{\int_0^\eta \exp\left[-Pr \int_0^\eta f d\eta\right] d\eta}{\int_0^\infty \exp\left[-Pr \int_0^\eta f d\eta\right] d\eta} \right] + \int_{r_1}^r \theta_{st}(r, z, r^*) \frac{dT_w(r^*)}{dr} dr^*. \quad (54)$$

The wall heat flux is

$$q_w = -k\sqrt{(3U_0/2\nu)r} \left\{ b \int_{r_1}^r \frac{1}{(1-r^*/r)^{1/3}} \times [F'_0(0) + F'_1(0)(1-r^*/r) + F'_2(0)(1-r^*/r)^2 + \dots] \frac{dT_w(r^*)}{dr} dr^* - \frac{T_w(r_1) - T_\infty}{\int_0^\infty \exp\left[-Pr \int_0^\eta f d\eta\right] d\eta} \right\} \quad (55)$$

and the Nusselt number is

$$Nu = \frac{Re^{1/2} \sqrt{(3d/2r)}}{T_w(r) - T_\infty} \left\{ \frac{T_w(r_1) - T_\infty}{\int_0^\infty \exp\left[-Pr \int_0^\eta f d\eta\right] d\eta} - b \int_{r_1}^r \frac{1}{(1-r^*/r)^{1/3}} [F'_0(0) + F'_1(0)(1-r^*/r) + F'_2(0)(1-r^*/r)^2 + \dots] \frac{dT_w(r^*)}{dr} dr^* \right\} \quad (56)$$

where  $F'_0(0)$ ,  $F'_1(0)$  and  $F'_2(0)$  are given by equations (24). For a Prandtl number smaller than unity, the thermal boundary layer reaches the free surface before

the viscous boundary layer does. Consequently, the present solution is valid in a smaller region if  $Pr < 1$ .

### 3.7. Solution for arbitrary wall heat flux

The temperature distribution in the boundary layer region for the case of arbitrary wall heat flux  $Q_w(r)$  and constant temperature  $T_\infty$  outside the boundary layer can be obtained by the superposition of equations (45) and (52) as follows:

$$T = T_\infty + \frac{Q_w(r_1)}{\sqrt{(3U_0/2\nu)k}} \theta_{ca} + \frac{1}{b\sqrt{(3U_0/2\nu)k}} \times \int_{r_1}^r (1-r^*/r)^{1/3} \theta_{ca}(r, z, r^*) \frac{dQ_w(r^*)}{dr} dr^* \quad (57)$$

The Nusselt number is obtained as

$$Nu = Re^{1/2} \sqrt{(3d/2r)Q_w(r)} \left\{ Q_w(r_1) \theta_{ca}(0) + \frac{1}{b} \int_{r_1}^r (1-r^*/r)^{1/3} [B_0(0) + B_1(0)(1-r^*/r) + B_2(0)(1-r^*/r)^2 + \dots] \frac{dQ_w(r^*)}{dr} dr^* \right\} \quad (58)$$

where  $B_0(0)$ ,  $B_1(0)$  and  $B_2(0)$  are given by equations (40).

Equations (56) and (58) give the Nusselt number profiles in the boundary layer region for prescribed wall temperature and wall heat flux, respectively. In the first part of this study, the Nusselt number profile in the vicinity of the stagnation point has been obtained. The integral solution in the transition region between the stagnation region and the boundary layer region is also obtained in the first part. Hence, one can plot the Nusselt number profile throughout the stagnation region and the boundary layer region. Since the asymptotic solution in the stagnation region is valid only for small values of  $r$  and the integral solution cannot be matched with the boundary layer region solution analytically, the solutions in different regions have to be matched graphically to obtain a continuous Nusselt number distribution. The procedure can be described as follows: first, the Nusselt number profiles near the stagnation point and in the boundary layer region are plotted, then we plot the Nusselt number profile in the transition region between the stagnation region and the boundary layer region. Finally, each segment of the curve is interpolated in such a way that the resulting curve is smooth everywhere. The results are shown in Figs. 8 and 9 for non-uniform wall temperature and wall heat flux, respectively.

In Figs. 8 and 9, the result of constant wall temperature and wall heat flux is compared with the result of increasing wall temperature and wall heat flux with  $r$ . The figures indicate that the Nusselt number for increasing wall temperature or wall heat flux is higher than that for constant wall temperature or wall heat

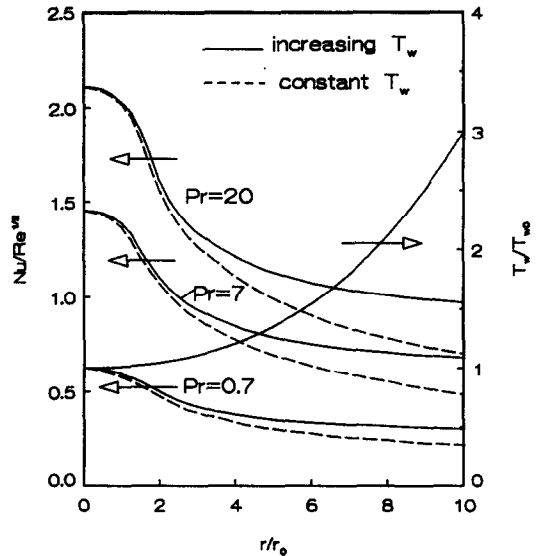


FIG. 8. Nusselt number profile for arbitrary wall temperature.

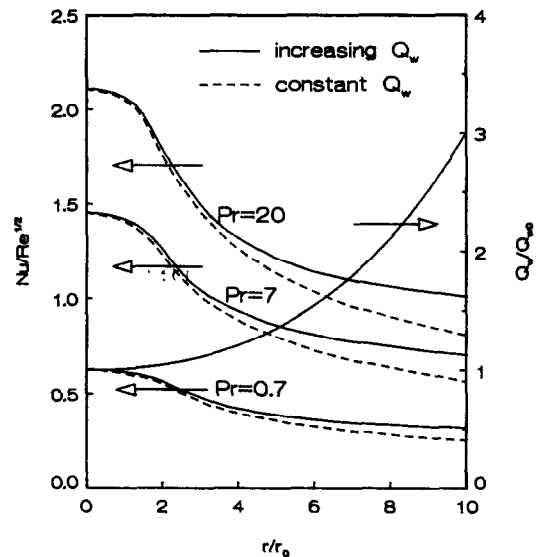


FIG. 9. Nusselt number profile for arbitrary wall heat flux.

flux outside the stagnation region. It can be seen from Figs. 8 and 9 that the Nusselt number near the stagnation point is essentially constant. At larger radial distance, however, the Nusselt number drops with  $r$  steeply. Very far away from the stagnation point, the Nusselt number decreases with  $r$  slowly.

The present result is compared with those obtained by Chaudhury [1] and Brdlik and Savin [3] in Fig. 10 for the case of constant wall temperature. The figure shows good agreement between the present result and Chaudhury's integral solution. For Brdlik and Savin's result, however, the Nusselt number is considerably higher than the present result and Chaudhury's result. This is because in ref. [3], the velocity at the outer edge of the boundary layer was assumed to be  $2U_0$ , where  $U_0$  is the jet velocity. If the velocity outside the bound-

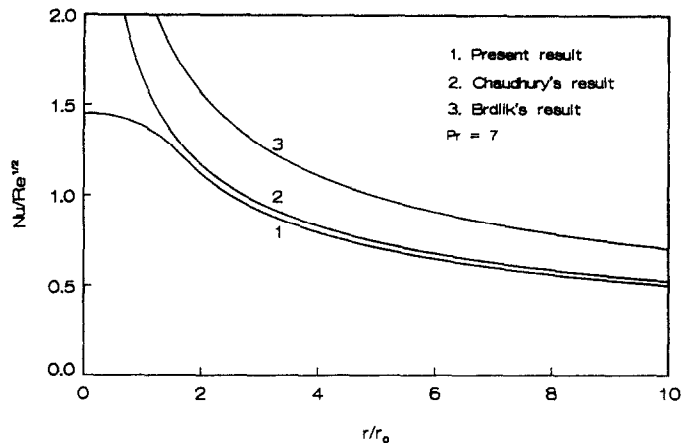


FIG. 10. Comparison with other results.

ary layer is taken to be  $U_0$  in ref. [3], the result will be in good agreement with the present solution and Chaudhury's solution.

#### 4. CONCLUSIONS

The heat transfer in the boundary layer region of an axisymmetrical jet impinging normally on a flat plate with non-uniform wall temperature or wall heat flux has been investigated analytically. The solution converges very fast for a Prandtl number of the order of unity or larger. For a very small Prandtl number, however, the solution may be divergent when  $R$  is not very small. In such a case, one may assume that the solution is semi-divergent and use Euler's transformation to evaluate the sum. The solution is matched with that in the stagnation region obtained in the first part of this study so that the Nusselt number distribution throughout the stagnation region and the boundary layer region is obtained.

The solution presented in this paper may be useful in some applications. It can be used to solve the conjugate problem in which an axisymmetrical jet impinges on the top surface of a solid plate with prescribed wall temperature or wall heat flux at the

bottom surface. The solution is also useful when one is considering the heat transfer of multi-jet impingement. With the Nusselt number distribution shown in the figures, it is clear that the distance between jets should not exceed about four jet diameters in order to obtain approximately uniform heat transfer.

#### REFERENCES

1. Z. H. Chaudhury, Heat transfer in a radial liquid jet, *J. Fluid Mech.* **20**, 501–511 (1964).
2. E. J. Watson, The radial spread of a liquid jet over a horizontal plane, *J. Fluid Mech.* **20**, 481–499 (1964).
3. P. M. Brdlik and V. K. Savin, Heat transfer between an axisymmetric jet and a plate normal to the flow, *J. Engng Phys.* **8**, 91–98 (1965).
4. N. R. Saad, W. J. M. Douglas and A. S. Mujumdar, Prediction of heat transfer under an axisymmetric laminar impinging jet, *Ind. Engng Chem. Fundam.* **16**, 148–154 (1977).
5. A. W. Lipsett and R. R. Gilpin, Laminar jet impingement heat transfer including the effects of melting, *Int. J. Heat Mass Transfer* **21**, 25–33 (1978).
6. K. Mitachi and R. Ishiguro, Heat transfer of wall jets (1st report: theoretical discussions of the temperature field), *Heat Transfer—Jap. Res.* **3**(4), 27–40 (1974).
7. B. T. Chao and L. S. Cheema, Forced convection in wedge flow with non-isothermal surfaces, *Int. J. Heat Mass Transfer* **14**, 1363–1375 (1971).

#### TRANSFERT THERMIQUE ENTRE UN JET CIRCULAIRE, LIBRE, INCIDENT ET UNE SURFACE SOLIDE AVEC TEMPERATURE PARIETALE OU FLUX DE CHALEUR PARIETAL NON UNIFORME—2. SOLUTION POUR LA REGION DE COUCHE LIMITE

**Résumé**—On étudie analytiquement le transfert thermique dans la région de couche limite pour un jet libre circulaire qui frappe une surface solide à température ou flux de chaleur non uniforme en paroi. L'écoulement est laminaire, incompressible et permanent. On obtient la solution du problème pour un changement en échelon de la température ou du flux. On obtient par superposition la solution du problème avec variation arbitraire de la température ou du flux. Cette solution est ensuite éprouvée avec celle de la région d'arrêt obtenue dans la première partie de l'étude, de façon à obtenir le nombre de Nusselt dans la région d'arrêt et dans la zone de couche limite. Les résultats montrent que le nombre de Nusselt pour une augmentation de température ou de flux à la paroi est considérablement plus grand que lorsque la température ou le flux reste uniforme en dehors de la région d'arrêt. Pour le cas particulier d'une température pariétale constante, le résultat est en bon accord avec la solution intégrale de Chaudhury.

WÄRMEÜBERTRAGUNG ZWISCHEN EINEM KREISFÖRMIGEN FREI  
AUFTREFFENDEN STRAHL UND EINER FESTEN OBERFLÄCHE MIT  
UNGLEICHFÖRMIGER WANDTEMPERATUR ODER WÄRMESTROMDICHTE—  
2. LÖSUNG FÜR DAS GRENZSCHICHTGEBIET

**Zusammenfassung**—Es wird der Wärmeübergang im Grenzschichtgebiet eines kreisförmigen freien Strahls bei Auftreffen auf eine ebene feste Oberfläche mit ungleichförmiger Wandtemperatur oder Wärmestromdichte analytisch untersucht. Die Strömung ist laminar, inkompressibel und stationär. Der erste Schritt der Betrachtung ist die Lösung des Problems bei einer stufenförmigen Änderung der Wandtemperatur oder Wärmestromdichte. Die Lösung für den Fall beliebiger Wandtemperatur oder Wärmestromdichte wird durch Überlagerung erhalten. Diese wird dann an die Lösung für das Stagnationsgebiet angepaßt, so daß die Nusselt-Zahl durchgehend vom Stagnations- bis zum Grenzschichtgebiet erhalten wird. Die Ergebnisse zeigen, daß die Nusselt-Zahl für zunehmende Wandtemperatur oder Wärmestromdichte beträchtlich größer sein kann als für konstante Wandtemperatur oder Wärmestromdichte außerhalb des Stagnationsbereiches. Für den Spezialfall konstanter Wandtemperatur stimmen die Ergebnisse gut mit der Integrallösung von Chaudhury überein.

ТЕПЛОПЕРЕНОС МЕЖДУ КРУГЛОЙ СВОБОДНО ПАДАЮЩЕЙ СТРУЕЙ И ТВЕРДОЙ  
ПОВЕРХНОСТЬЮ С НЕОДНОРОДНЫМ РАСПРЕДЕЛЕНИЕМ ТЕМПЕРАТУРЫ ИЛИ  
ТЕПЛООВОГО ПОТОКА—2. РЕШЕНИЕ ДЛЯ ОБЛАСТИ ПОГРАНИЧНОГО СЛОЯ

**Аннотация**—Аналитически исследуется теплоперенос в области пограничного слоя для круглой струи, свободно падающей на плоскую твердую поверхность с неоднородным распределением температуры и теплового потока. Течение является ламинарным, несжимаемым и стационарным. Анализ начинается с получения решения задачи со скачкообразным изменением температуры или теплового потока на стенке. Методом суперпозиции получено решение соответствующей задачи для произвольных температуры-или теплового потока на стенке. Данное решение затем согласовывается с решением для области торможения, полученным в первой части исследования, с целью определения числа Нуссельта по всей зоне торможения и пограничного слоя. Результаты показывают, что для возрастающих на стенке температуры или теплового потока число Нуссельта может быть значительно выше, чем для постоянных за пределами зоны торможения. Результаты для частного случая постоянной температуры стенки хорошо согласуются с интегральным решением Чаудхури.